HHS Public Access

Author manuscript

J Vasc Interv Radiol. Author manuscript; available in PMC 2016 October 04.

Published in final edited form as:

J Vasc Interv Radiol. 2015 December ; 26(12): 1887–94.e1. doi:10.1016/j.jvir.2015.01.014.

Calibrated Bioresorbable Microspheres as an Embolic Agent: An Experimental Study in a Rabbit Renal Model

Lihui Weng, PhD, **Davis Seelig, DVM, PhD**, **Parinaz Rostamzadeh, BS**, and **Jafar Golzarian, MD**

Department of Radiology (L.W., P.R., J.G.), University of Minnesota, Mayo B228, 420 Delaware Street SE, Minneapolis, MN 55455; and Department of Veterinary Clinical Sciences (D.S.), University of Minnesota, St Paul, Minnesota

Abstract

Purpose—To evaluate the time frame of resorption and tissue response of newly developed bioresorbable microspheres (BRMS) and vessel recanalization after renal embolization.

Materials and Methods—Embolization of lower poles of kidneys of 20 adult rabbits was performed with BRMS (300–500 μm). Two rabbits were sacrificed immediately after embolization (day 0). Three rabbits were sacrificed after follow-up angiography at 3, 7, 10, 14, 21, and 30 days. The pathologic changes in the renal parenchyma, BRMS degradation, and vessel recanalization were evaluated histologically and angiographically.

Results—Embolization procedures were successfully performed, and all animals survived without complication. Infarcts were observed in all kidneys that received embolization harvested after day 0. Moderate degradation of BRMS (score = 1.07 ± 0.06) was observed by day 3. Of BRMS, 95% were resorbed before day 10 with scant BRMS materials remaining in the arteries at later time points. Partial vessel recanalization was observed by angiography starting on day 3, whereas new capillary formation was first identified histologically on day 7. Vascular inflammation associated with BRMS consisted of acute, heterophilic infiltrate at earlier time points (day 3 to day 10); this was resolved with the resorption of BRMS. Inflammation and fibrosis within infarcted regions were consistent with progression of infarction.

Conclusions—BRMS were bioresorbable in vivo, and most BRMS were resorbed before day 10 with a mild tissue reaction. Vessel recanalization occurred secondary to the resorption of BRMS.

Bioresorbable particles offer potential advantages over nonresorbable particles for embolization. First, their resorbability makes them more favorable than comparable nonresorbable materials that persist in vivo with unknown consequences. Second, the transient nature of embolization produced by resorbable embolic agents would allow for repeat procedures in oncologic indications (1). The resorption would result in limited hypoxia, which can reduce tumor angiogenesis (2). Lastly, for chemoembolization with

Address correspondence to J.G.; jafar@umn.edu.

L.W. and J.G. are owners or shareholders in EmboMedics, Inc. They hold a patent on the microspheres used in this study. Neither of the other authors has identified a conflict of interest.

Figure E1 is available online at www.jvir.org.

drug-eluting microspheres, the drug would be completely released by the time of resorption of bioresorbable microspheres. Increased tissue necrosis has been observed in chemoembolization with doxorubicin-loaded nonresorbable microspheres (DC Bead; Biocompatibles UK Ltd, Farnham, Surrey, United Kingdom) because of the long-term presence of the microspheres containing doxorubicin (3).

Current commercially available bioresorbable embolic materials include gelatin sponge (Gelfoam; Pfizer, Inc, New York, New York) and starch microspheres (Embo-Cept® S; PharmaCept, Berlin, Germany), both of which have shortcomings. The gelatin sponge available in the United States is nonspherical and requires manual cutting, which results in size discrepancy and variable levels of occlusion (4). The degradation of gelatin sponge is unpredictable. Although resorption of gelatin sponge has been reported to occur typically 7 and 21 days after embolization (5), some reports have shown a high percentage of permanent vessel occlusion with gelatin sponge (6,7). Starch microspheres are calibrated and can be used to deliver chemotherapeutic drugs in liver tumors (8). However, they are available in only one small caliber (~50 μm) and have a very short half-life (~40 min).

Calibrated bioresorbable microspheres (BRMS) were developed to address the aforementioned concerns (9). These microspheres are made of natural polysaccharides and possess excellent cell compatibility, hydrophilicity, and in vitro degradability that can be readily adjusted by modulating their composition (10). In vivo resorbability of BRMS has been confirmed in a rabbit renal model (10). Although these preliminary studies have shown that BRMS are promising for embolization (9,10), their time frame of resorption and related features are unknown. The aim of the present study was to determine the time frame of resorption, tissue response, and kinetics of vessel recanalization using BRMS in a rabbit renal model.

Materials and Methods

Microspheres

BRMS were prepared from 2% (weight/volume) oxidized carboxymethylcellulose (theoretical oxidation degree of 25%) and 2% (weight/volume) carboxymethyl chitosan aqueous solutions by an inverse emulsion method (10). Calibrated BRMS of 300–500 μm were obtained by sieving BRMS with US standard sieves, and sieved microsphere size distribution was assessed with an optical microscope (Olympus CK-2; Olympus Corporation, Shinjuku-ku, Tokyo, Japan) by measuring the diameters of 200 randomly picked microspheres. The concentration of the microsphere suspension used was 10 mg/mL in a 5:5 saline:contrast (Optiray 320; Mallinckrodt Inc., Hazelwood, Missouri) mixture.

Embolization of the Renal Artery

All experiments had institutional animal care and use committee approval. In this study, 20 adult rabbits (New Zealand white) weighing 2.9–3.3 kg were used. Two rabbits received embolization in the lower pole of both kidneys and were sacrificed immediately after embolization. The remaining 18 rabbits received BRMS in the lower pole of one kidney and were divided into six groups of three animals each according to the time of euthanasia (day

3, 7, 10, 14, 21, and 30). Rabbits were anesthetized by intramuscular administration of ketamine hydrochloride (35 mg/kg), xylazine (5 mg/kg), and acepromazine (0.75 mg/kg). Each rabbit was intubated, and general anesthesia was maintained with 1.5%–2% isoflurane and 1 L/min oxygen. The right common femoral artery was surgically exposed, and a 4-F sheath was placed. Under fluoroscopic guidance, the renal artery was catheterized with a 4-F Cobra catheter (internal diameter = 0.038 inch) (Glidecath; Terumo Medical Corp, Somerset, New Jersey), inside which a 2.7-F microcatheter (internal diameter = 0.025 inch) (Progreat; Terumo Medical Corp) was placed. BRMS were delivered through the microcatheter into the lower pole of the kidneys at a rate of ~1 mL/min to achieve stasis, and the volume of the microsphere suspension administered was recorded. Angiography was performed before and after embolization. The arterial access site was closed by ligation.

Follow-up Angiography and Histopathology

At each sacrifice time point, rabbits underwent angiography, and the recanalization rate was estimated by comparing the opacified arteries on final angiograms with arteries on angiograms obtained immediately after embolization (4). The rabbits were euthanized by intravenous injection of a barbiturate-based euthanasia solution (Euthasol; Virbac Animal Health, Fort Worth, Texas). Each harvested kidney was divided into three blocks, 3- to 4-mm, representing anterior, middle, and posterior regions. The infarct volume percentage of each kidney was calculated by measuring the infarcted area and total area of the kidney blocks and multiplying areas by thickness of the affected tissue (11). Kidney blocks were fixed in 10% phosphate-buffered formalin, routinely processed, and embedded in paraffin. Two 5-μm-thick sections were trimmed from each paraffin block and stained with hematoxylin and eosin. In addition, selected sections were stained with Masson trichrome and Verhoeff-van Gieson elastin stains to evaluate for fibrosis and the status of the internal elastic lamina (IEL) of vessel walls, respectively.

Microscopic evaluation focused on the effects of BRMS on vessels and the surrounding renal tissue. Each stained section was examined for (*a*) the presence of microspheres or microsphere fragments, (*b*) microsphere resorption, (*c*) arterial location of microspheres, (*d*) coagulative necrosis, (*e*) heterophilic inflammation, (*f*) mononuclear inflammation, (*g*) granulomatous (foreign body–type) inflammation, (*h*) neointimal hyperplasia, (*i*) recanalization, (*j*) thrombus organization, (*k*) damage to the IEL, and (*l*) fibrosis (12). Pathologic features were generally qualitatively (absent, mild, moderate, and marked) graded unless specified; some were semi-quantitatively graded (described subsequently). When applicable, the pathologic feature was defined according to the level of the renal arterial tree affected (ie, interlobar, arcuate, or interlobular arteries) by focusing on the most severely affected tissue area or vessel from each tissue section. All slides were evaluated by a board-certified veterinary pathologist (D.S.) blinded to the treatment each group received.

The presence of microspheres or fragments in the arteries was qualitatively described as most (70%–100%), many (40%–70%), a few (5%–40%), rare (1%–5%), and single fragment (< 1%), where the average number of microspheres per kidney identified at day 0 was considered as 100%. Microsphere resorption was scored using the following 5-point scale (13): 0, original spherical shape and size maintained, or a slight deformation; 1, moderately

evident size reduction and distortion of the particle and cleft or cavity formation within the particle; 2, clearly evident size reduction and distortion of the particle and the cleft or cavity formation; 3, only scant microsphere material observed; or 4, no microsphere observed. Coagulative necrosis was defined as areas of renal parenchyma demonstrating loss of nuclear and cell detail but retention of architecture. The three inflammatory patterns (heterophilic, mononuclear, and granulomatous/foreign body–type) were defined by infiltration of renal parenchyma, vessels, or both by a characteristic cell type (heterophils, lymphocytes and plasma cells, or macrophages and multinucleate giant cells) and graded according to severity. Specifically, vascular inflammation associated with BRMS was semiquantitatively graded as follows: 1, mild focal or multifocal perivascular or intravascular infiltrate of inflammatory cells without evidence of vascular necrosis; 2, moderate perivascular or intravascular infiltrate of inflammatory cells with or without limited evidence of vascular necrosis; or 3, severe perivascular or intravascular infiltrate (multifocal aggregates) of inflammatory cells with some vascular necrosis. When identified, thrombi were characterized regarding their degree of organization, which reflects the progressive infiltration of the original fibrin clot by collagen-secreting fibroblasts and transformation into fibrovascular tissue. Neointimal hyperplasia was defined as thickening of the intimal layer secondary to increased cellular and matrix density. Recanalization was defined as the formation of newly developed vascular structures within a vessel after embolization and graded according to the degree to which the original vessel luminal diameter was restored as absent, mild (up to 33% of the original lumen was restored), moderate (restoration of 34%–66% of the original luminal diameter), or marked (restoration of 67%–100% of the original vessel luminal diameter). Lastly, disruption of the vascular IEL was graded as follows: absent (intact IEL), mildly damaged (1%–33% of the IEL was destroyed), moderately damaged (34%–66% of the IEL was destroyed), or markedly damaged (67%–100% of the IEL was destroyed).

Statistical Analysis

Data were summarized using the mean and SD for numeric variables. Multiple comparisons between groups were evaluated by analysis of variance. Difference was considered significant if P was < .05. Data were analyzed using SAS version 9.3 (SAS Institute, Cary, North Carolina).

Results

Embolic Materials

By light microscopy, BRMS were globular in shape with minimal defects (Fig 1). The average diameter of the microspheres was 407 μm ± 57 with a range of 300-500 μm (Fig E1 [available online at www.jvir.org]).

Renal Arterial Intervention and Angiography

BRMS embolization was successfully performed in all rabbits without clogging. The mean volume of BRMS injected per kidney was 1.64 mL ± 0.91. Angiography (Fig 2a–c) confirmed embolization of the lower pole of kidneys to stasis on day 0 (Fig 2b). All animals survived to sacrifice without complications.

At follow-up angiography, complete vessel occlusion was maintained for two of the three kidneys that received embolization on day 3, and flow was partially recovered for one kidney that received embolization (< 10%). On day 7, partial reperfusion was observed in two of the three kidneys that received embolization (> 70%), whereas one kidney that received embolization was totally reperfused. On day 10, two of the three kidneys that received embolization were totally reperfused (Fig 2c), and the remaining was nearly completely reperfused (> 80%). From day 14 to day 30, all kidneys were reperfused.

Macroscopic Evaluation

Kidneys of the animals sacrificed immediately after embolization showed no evidence of infarct but demonstrated reddish brown mottling on the surface. For animals sacrificed at later time points, all kidneys showed regionally extensive areas of acute infarction reflected by white-grayish discoloration on the external surfaces of the lower pole and multiple peripheral wedge-shaped lesions on the cut surface. There was no evident size reduction in the kidneys after embolization compared with control kidneys. The average infarct volumes of the kidneys after embolization were 4%–13% with smaller infarct volumes observed at later time points compared with earlier time points. However, the difference was not significant ($P = .43$, analysis of variance).

Microscopic Histopathology Findings

The pathologic findings are summarized in Tables 1 and 2. In the hematoxylin-eosin–stained sections, BRMS had a characteristic dark pink to red color (Fig 3a–e). On day 0, BRMS were located at interlobar and arcuate arteries without obvious deformation or size reduction (score = 0) (Table 1 and 2, Fig 3a). From day 3 to day 7, BRMS were found in all three arterial levels (interlobar, arcuate, and interlobular) with 40%–70% of microspheres remaining compared with day 0 (Table 1). The first sign of microsphere resorption was identified on day 3 as evidenced by a moderate size reduction with irregular borders (Table 2, Fig 3b). On day 7, microspheres were identified with a clear size reduction (Table 2, Fig 3c). On day 10 and day 14, few microsphere fragments (≤ 5%) were identified in interlobular arteries in only one of the three kidneys that received embolization (Table 1 and 2, Fig 3d, e). On day 21 and day 30, only a single small fragment (< 1%) of BRMS was identified in interlobular arteries (Tables 1, 2). Of BRMS, 95% were resorbed before 10 days, and there was a significant change in the microsphere morphology over the whole study period ($P < .00001$, analysis of variance).

Starting on day 3 and extending to day 30, multiple areas of predominantly cortical infarction were identified. In these areas, the necrosis was largely coagulative, with scant inflammation and mineralization at later time points (Table 1). Inflammation was identified at all time points except immediately after embolization (Fig 3a–f). Early in the study (days 3 and 7) (Fig 3b, c), inflammation was predominantly heterophilic with inflammatory cells centered on renal arteries that received embolization and at the edges of the areas of infarction. However, starting at day 7 and persisting to day 30, the inflammatory infiltrate became increasingly mononuclear (ie, dominated by lymphocytes and macrophages) with aggregates of multinucleated giant cells and evidence of microsphere resorption. Coincident with this increase in mononuclear inflammatory cells, a decline in proportion of heterophils

and a progressive increase in fibrosis were observed. When only the vascular inflammation was evaluated, a similar pattern emerged. Similar to the tissue inflammation, the vascular inflammation was predominantly heterophilic (Fig 3b) early in the study with small numbers of multinucleate giant cells. Semiquantitative analysis of the vascular inflammation revealed that its severity peaked at day 10 and dramatically declined by day 14 and never became more than mild to moderate. In addition, vascular inflammation was limited to the area immediately adjacent to microspheres, and severity of vascular inflammation decreased as microsphere resorption advanced (Table 2).

Elastin staining confirmed vascular injury through the identification of neointimal hyperplasia and disruption of the IEL over the study period. Neointimal hyperplasia, a nonspecific indicator for vessel injury, was first identified on day 7 (Fig 4a) and persisted, in varying severity, through the duration of the study. Similarly, disruption of the IEL was first identified on day 3, increased on day 7, and remained relatively static over the remainder of the study (Table 1, Fig 4b).

The organization of thrombi and recanalization were first identified on day 7 and persisted through the duration of the study (Fig 4b, d). At later time points, the occluded vessels showed mild inflammation with or without scant microsphere materials (Fig 3e). The recanalized vessels showed a thickened media or intima (Fig 3f). Masson trichrome staining revealed evidence of mild fibrosis on day 3, which increased over the course of the study (Fig 4c, d). The fibrosis was most pronounced within, and immediately adjacent to, the areas of parenchymal infarction and necrosis, although there were occasional foci of periarteriolar fibrosis.

Discussion

BRMS are injectable, degradable, variably sized (50– 1,200 μm), and drug-loadable polymer microspheres (9,10) with a modifiable in vitro survivability profile that can range from 7 days to several months by modulating their cross-linking degree (10). The present study demonstrates the safety and ease of using BRMS as an embolic agent. The presence of infarcts confirmed that this material achieves the desired goal of embolization similar to commercially available nonresorbable embolic materials (11,14). Similar to previous studies (15), the BRMS in rabbits sacrificed on day 0 were identified in the interlobar and arcuate arteries, although the level of occlusion changed as the resorption continued. Ohta et al (13) described a similar phenomenon in which gelatin microspheres > 100 μm progressively migrated from the interlobar arteries to interlobular arteries, which was much faster than BRMS. The gradual distal migration of the BRMS in this study is likely related to their progressive degradation and associated decreased size and altered compressibility. This migration is inherent to resorbable materials and is unlikely to cause any potential clinical problem based on the clinical studies with gelatin sponge (6,7).

Of BRMS, 95% were resorbed before day 10 with scant fragments observed at later time points, which is much faster than their in vitro enzymatic degradation (9). This difference likely reflects the remarkably different in vivo environment, where body fluids (eg, blood), enzymes, and infiltrating inflammatory cells are involved, compared with in vitro conditions.

In addition, a partial occlusion of the kidney was performed in the present study, and the extent of BRMS degradation at day 3 was comparable to that at day 7 in another study where a total occlusion of the kidney was performed (10). This finding suggests that a partial occlusion of the kidney results in more rapid microsphere degradation because residual blood flow facilitates the delivery of inflammatory cells and proinflammatory substances. These findings support the idea that BRMS are resorbed through hydrolysis and phagocytosis, similar to the intra-arterial degradation of pure chitosan microspheres (12).

The endpoint of embolization regulates not only resorption but also inflammation and vascular damage. Collaterals and viable tissue adjacent to the vessels that receive embolization are necessary to initiate the inflammation reaction. In a typical response to a foreign material, the number of macrophages in the area surges almost immediately, peaks at day 3 to day 4, and begins to subside at day 6 to day 7 (16). In the present study, the vascular inflammation associated with BRMS peaked at day 7 to day 10 and then subsided with the resorption of BRMS. In addition, vascular injury, as reflected by disruption of the IEL, was observed. In contrast, Kwak et al (12) demonstrated an intact hilar renal arterial IEL in rabbit kidneys 4 weeks after embolization with chitosan microspheres. We propose that differences in embolization completeness are primarily responsible for these disparate findings. That is, the total occlusion of the kidney obtained by Kwak et al (12) limited or prohibited renal blood flow, which prevented inflammatory cell ingress and ultimately blunted any resulting vascular injury. Support for this hypothesis is illustrated by findings in a study using BRMS to obtain complete occlusion of the kidney, in which no inflammation was identified on days 6 or 7 and vessels demonstrated an intact IEL (10). In addition, BRMS are calibrated and traditionally have a better inflammatory profile despite IEL disruption than gelatin sponge (17).

Compared with nonresorbable microspheres, BRMS are bioresorbable, while still achieving a similar level of occlusion (15). Owing to their resorbability, it is reasonable to anticipate that the inflammation associated with BRMS is inherently self-limiting. That is, progressive degradation and eventual complete removal of the foreign material, in conjunction with restoration of blood flow (both of which are illustrated in our work), will ameliorate the inflammation. In contrast, nonresorbable microspheres are permanent, and the foreign body reaction is present for their in vivo lifetime (18).

Progressive fibrosis, which increased from day 3 to day 30, was another major finding in this study. A similar finding was described in a study (13) in which gelatin microsphere embolization of the rabbit kidney resulted in progressive fibrosis from day 3 to day 14. Lastly, destruction of the IEL has previously been reported with gelatin sponge and nonresorbable microspheres (11,14), indicating this reaction is not unusual for arterial embolization with existing commercially available embolic materials.

As part of the embolization process, thrombosis and progressive recanalization were identified. The rate of thrombus organization is related in part to the magnitude of the inflammation induced by the embolic agent (ie, the more severe the inflammation, the more rapid the thrombus organization) (19). If the rate of thrombolysis exceeds the rate of organization, vessel recanalization occurs. In the present study, the organization of thrombi

and formation of new capillaries (recanalization) were first identified on day 7, although the partial reperfusion of the vessels that received embolization was observed early on day 3 angiographically. The formation of capillaries was observed more frequently at later time points, which is consistent with angiography. BRMS achieved vessel recanalization sooner than degradable hydroxyethyl acrylated microspheres (20) but more slowly than water-soluble polyvinyl alcohol microspheres (21). In addition, polyethylene glycol hydrogel microspheres with a resorption time shorter than BRMS were shown to reach a total recanalization at day 7 based on angiography (5,22). The ideal occlusion time is unknown and may depend on the indication and location of the target vessel or organ.

This study has some limitations. First, only two sections per block (anterior, middle, and posterior) were examined. In some cases, the area of impaction of the microspheres may have not been included in the section. Second, histologic sectioning may underestimate the size of microspheres, which may affect the degradation score. Third, the method used to estimate the infarction volume based on area and thickness measurement may bring subjectivity to this study. Fourth, the determination of recanalization rate was based on angiography, which can bring subjectivity to the results because of the difficulty in visually identifying distal small arteries on angiograms.

In conclusion, this renal embolization study demonstrated that BRMS are resorbable with mild tissue reaction and that vessel recanalization and restoration occurred after the resorption of BRMS. Future studies are needed to evaluate the resorption of BRMS in the liver model of larger animals and the effect of drug loading on the resorption.

Supplementary Material

Refer to Web version on PubMed Central for supplementary material.

Acknowledgments

The project was supported by a pilot research grant (L.W., 2011, No. 001612) from the Society of Interventional Radiology Foundation.

References

1. Brown DB, Pilgram TK, Darcy MD, et al. Hepatic arterial chemoembolization for hepatocellular carcinoma: comparison of survival rates with different embolic agents. J Vasc Interv Radiol. 2005; 16:1661–1666. [PubMed: 16371533]
2. Zhou B, Wang J, Yan Z. Ginsenoside Rg3 attenuates hepatoma VEGF overexpression after hepatic artery embolization in an orthotopic transplantation hepatocellular carcinoma rat model. Onco Targets Ther. 2014; 7:1945–1954. [PubMed: 25364265]
3. Namur J, Citron SJ, Sellers MT. Embolization of hepatocellular carcinoma with drug-eluting beads: doxorubicin tissue concentration and distribution in patient liver explants. J Hepatol. 2011; 55:1332–1338. [PubMed: 21703190]
4. Maeda N, Verret V, Moine L, et al. Targeting and recanalization after embolization with calibrated resorbable microspheres versus hand-cut gelatin sponge particles in a porcine kidney model. J Vasc Interv Radiol. 2013; 24:1391–1398. [PubMed: 23891049]
5. Barth KH, Strandberg JD, White RI Jr. Long term follow-up of transcatheter embolization with autologous clot, oxycel and gelfoam in domestic swine. Invest Radiol. 1977; 12:273–280. [PubMed: 863632]

6. Jander J, Russinovich N. Transcatheter gelfoam embolization in abdominal, retroperitoneal, and pelvic hemorrhage. Radiology. 1980; 136:337–344. [PubMed: 6967615]
7. Geschwind JF, Ramsey D, Cleffken B, et al. Transcatheter arterial chemoembolization of liver tumors: effects of embolization protocol on injectable volume of chemotherapy and subsequent arterial patency. Cardiovasc Intervent Radiol. 2003; 26:111–117. [PubMed: 12616414]
8. Yamasaki T, Saeki I, Harima Y, et al. Effect of transcatheter arterial infusion chemotherapy using iodized oil and degradable starch microspheres for hepatocellular carcinoma. J Gastroenterol. 2012; 47:715–722. [PubMed: 22322658]
9. Weng L, Le H, Talaie R, Golzarian J. Bioresorbable hydrogel microspheres for transcatheter embolization: preparation and in vitro evaluation. J Vasc Interv Radiol. 2011; 22:1464–1470. [PubMed: 21816624]
10. Weng L, Rostamzadeh P, Nooryshokry N, Le HC, Golzarian J. In vitro and in vivo evaluation of biodegradable embolic microspheres with tunable anticancer drug release. Acta Biomater. 2013; 9:6823–6833. [PubMed: 23419554]
11. Siskin GP, Dowling K, Virmani R, Jones R, Todd D. Pathologic evaluation of a spherical polyvinyl alcohol embolic agent in a porcine renal model. J Vasc Interv Radiol. 2003; 14:89–98. [PubMed: 12525592]
12. Kwak BK, Shim HJ, Han SM, Park ES. Chitin-based embolic materials in the renal artery of rabbits: pathologic evaluation of an absorbable particulate agent. Radiology. 2005; 236:151–158. [PubMed: 15987971]
13. Ohta S, Nitta N, Takahashi M, Murata K, Tabata Y. Degradable gelatin microspheres as an embolic agent: an experimental study in a rabbit renal model. Korean J Radiol. 2007; 8:418–428. [PubMed: 17923785]
14. Bilbao JI, de Luis E, García de Jalón JA, et al. Comparative study of four different spherical embolic particles in an animal model: a morphologic and histologic evaluation. J Vasc Interv Radiol. 2008; 19:1625–1638. [PubMed: 18823795]
15. Weng L, Rusten M, Talaie R, Hairani M, Rosener NK, Golzarian J. Calibrated bioresorbable microspheres (BRMS): a preliminary study on the level of occlusion and arterial distribution in a rabbit kidney model. J Vasc Interv Radiol. 2013; 24:1567–1575. [PubMed: 23928298]
16. Enoch S, Leaper DJ. Basic science of wound healing. Surgery. 2005; 23:37–42.
17. Goldstein HM, Wallace S, Anderson JH, Bree RL, Gianturco C. Transcatheter occlusion of abdominal tumors. Radiology. 1976; 120:539–545. [PubMed: 948584]
18. Stampfl U, Stampfl S, Bellemann N, et al. Experimental liver embolization with four different spherical embolic materials: impact on inflammatory tissue and foreign body reaction. Cardiovasc Intervent Radiol. 2009; 32:303–312. [PubMed: 19139955]
19. Sniderman KW, Sos TA, Alonso DR. Transcatheter embolization with Gelfoam and Avitene: the effect of Sotradecol on the duration of arterial occlusion. Invest Radiol. 1981; 16:501–507. [PubMed: 7319757]
20. Schwarz A, Zhang H, Metcalfe A, Salazkin I, Raymond J. Transcatheter embolization using degradable crosslinked hydrogels. Biomaterials. 2004; 25:5209–5215. [PubMed: 15109845]
21. Shomura Y, Tanigawa N, Shibutani M, et al. Water-soluble polyvinyl alcohol microspheres for temporary embolization: development and in vivo characteristics in a pig kidney model. J Vasc Interv Radiol. 2011; 22:212–219. [PubMed: 21194968]
22. Verret V, Pelage JP, Wassef M, et al. A novel resorbable embolization microsphere for transient uterine artery occlusion: a comparative study with trisacryl-gelatin microspheres in the sheep model. J Vasc Interv Radiol. 2014; 25:1759–1766. [PubMed: 25194456]

Abbreviations

BRMS	bioresorbable microspheres
IEL	internal elastic lamina

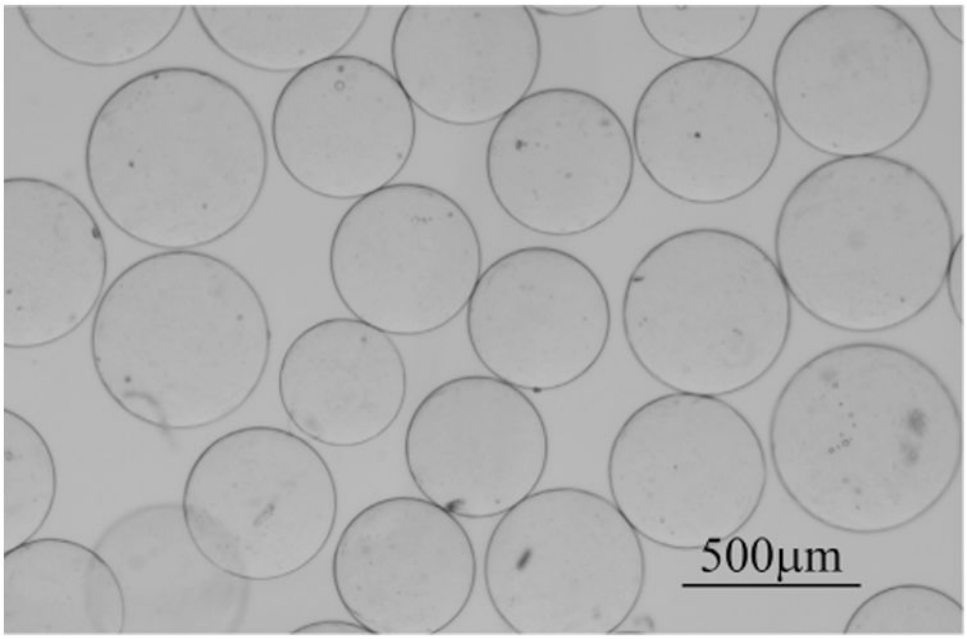

Figure 1.
Microscopic image of 300–500 μm BRMS.

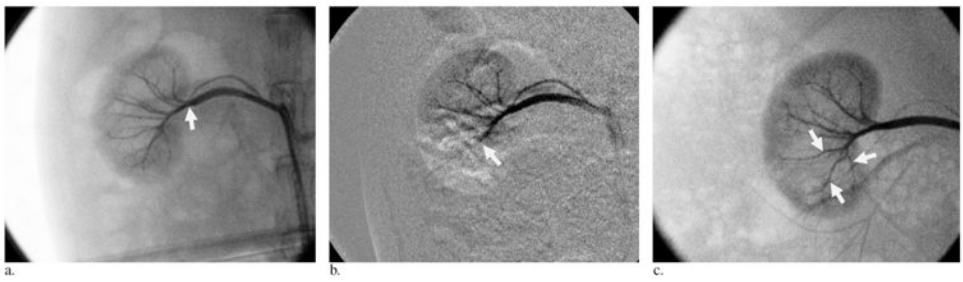

Figure 2.

Example of renal artery recanalization after embolization with BRMS. (**a**) Angiogram obtained before embolization. Renal arteries (arrow) are opacified. (**b**) Angiogram obtained immediately after embolization. Embolization of the arterial branch (arrow) into the lower pole of the kidney was performed. (**c**) Angiogram obtained on day 10. Right renal angiogram shows reperfusion of the arteries that received embolization (arrows).

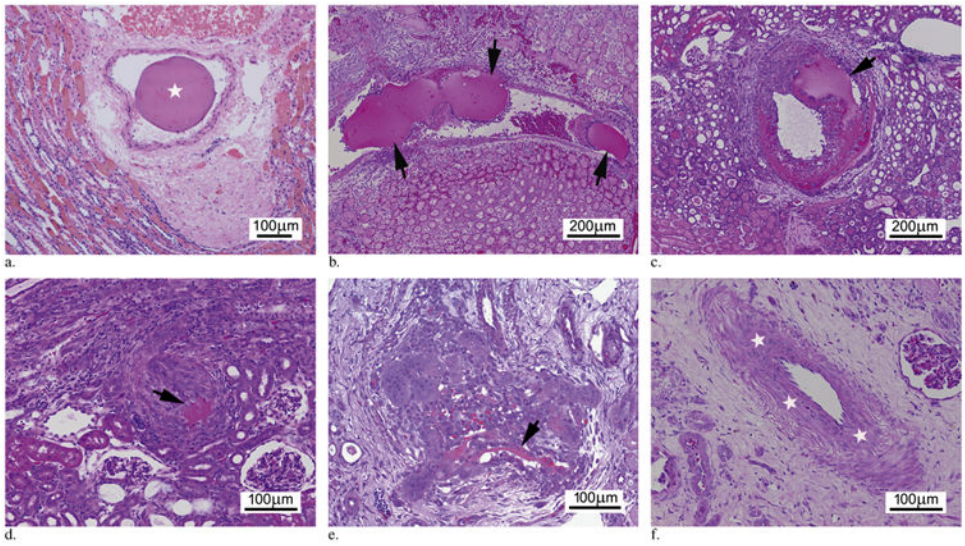

Figure 3.

Progressive intra-arterial microsphere resorption. (**a**) Day 0. Photomicrograph demonstrates a single BRMS (star) within the arterial lumen with no evidence of degradation (score 0). (**b**) Day 3. Photomicrograph demonstrates several intra-arterial BRMSs (arrows) with moderate size reduction (score 1). (**c**) Day 7. Photomicrograph illustrates BRMS (arrow) in the artery with clearly evident size reduction (score 2) accompanied by cell infiltration. (**d**) Day 10. Photomicrograph demonstrates only a single remnant fragment of BRMS (arrow) in the artery (score 3). (**e**) Day 14. Photomicrograph shows remnants of BRMS (arrow) within an artery (score 3). (**f**) Day 21. Photomicrograph shows recanalized vessels with thickened media (stars). (Available in color online at www.jvir.org.)

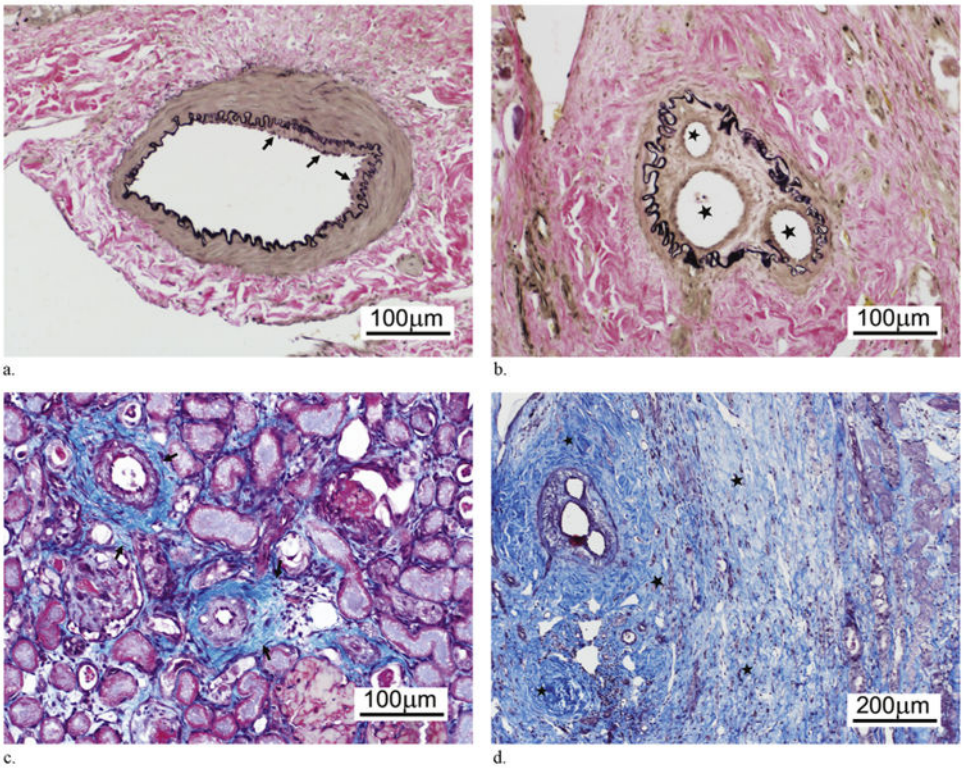

Figure 4.

Renal pathology after BRMS embolization. (**a**) Photomicrograph demonstrates mild neointimal hyperplasia (arrows) at day 7 (elastin staining). (**b**) Photomicrograph demonstrates evidence of intra-arterial recanalization with new vascular channels (stars) formed on day 21 (elastin staining). (**c**) Photomicrograph illustrates mild to moderate interstitial fibrosis (arrows) on day 7 (Masson trichrome staining). (**d**) Photomicrograph demonstrates marked interstitial fibrosis (stars) adjacent to the recanalized vessel on day 21 (Masson trichrome staining). (Available in color online at www.jvir.org.)

Table 1

Summary of Microscopic Pathologic Findings in Rabbit Kidneys after Embolization with BRMS

Pathologic Finding	Day 0	Day 3	Day 7	Day 10	Day 14	21 d	30 d
BRMS present	Most	Many	Many (fragments)	Rare (fragments)	Rare (fragments)	Single fragment	Single fragment
BRMS arterial location	Interlobar-arcuate	Interlobar-arcuate-interlobular	Interlobar-arcuate-interlobular	Interlobular	Interlobular	Interlobular	Interlobular
Coagulative necrosis	Absent	Mild to moderate	Moderate to marked	Mild to moderate	Mild to moderate	Mild to moderate	Mild to moderate
Heterophilic inflammation	Absent	Moderate to marked	Moderate	Absent	Absent	Absent	Absent
Mononuclear inflammation	Absent	Mild	Moderate	Mild to moderate	Mild	Mild	Mild to moderate
Granulomatous/foreign body–type inflammation	Absent	Mild	Mild	Mild	Mild to moderate	Mild	Mild
Neointimal hyperplasia	Absent	Absent	Mild	Moderate to severe	Mild to moderate	Mild to moderate	Mild
Recanalization	Absent	Absent	Minimal	Mild	Mild to moderate	Mild to moderate	Mild
Fibrosis	Absent	Minimal	Mild to moderate	Moderate to marked	Moderate	Moderate to marked	Moderate to marked
Disruption of IEL	Absent	Mild to moderate	Moderate to marked	Moderate	Moderate to marked	Moderate to marked	Moderate

BRMS = bioresorbable microspheres, IEL = internal elastic lamina.

Table 2

Scores of Microsphere Resorption and Vascular Inflammation

Day	Microsphere Resorption Score (Average ± SD)	Vascular Inflammation Score (Average ± SD)
0	0	0
3	1.07 ± 0.06	0.89 ± 0.53
7	2.21 ± 0.22	1.17 ± 0.47
10	3.25 ± 0.33	1.22 ± 0.33
14	3.28 ± 0.32	0.33 ± 0.35
21	3.67 ± 0.29	0.33 ± 0.25
30	3.67 ± 0.29	0.33 ± 0.25